Journal of Structural Geology, Vol. 15, No. 6, pp. 737 to 751, 1993
Printed in Great Britain

0191-8141/93 $06.00+0.00

The origin and spacing of cross joints: examples from the Monterey Formation, Santa Barbara Coastline, California

MICHAEL R. GROSS

Department of Geosciences, Pennsylvania State University, University Park, PA 16802, U.S.A.

(*Received* 28 *October* 1991; *accepted in revised form* 3 *August* 1992)

Abstract—Cross joints in the Monterey Formation terminate against a series of pre-existing systematic strike-perpendicular joints. The strike-perpendicular joints act as mechanical layer boundaries during cross joint propagation, and the distance between adjacent strike-perpendicular joints represents a mechanical layer thickness. The fracture spacing index (FSI), or ratio of joint-controlled mechanical layer thickness to cross joint spacing in the Monterey Formation, is approximately 1.3. A model is proposed for cross joint propagation based on the analysis of stress reduction in the vicinity of a newly-formed joint. In this model, cross joint development follows a sequential infilling process as remote tensile stress increases with time. According to the model, the first cross joints (FSI = 0.32) propagate under a remote tensile stress of approximately −14 MPa. A second episode of cross jointing (FSI = 0.65) initiates when remote tensile stress reaches −27 MPa, and a third generation of cross joints (FSI = 1.30) develops at −57 MPa. Joints in each successive episode initiate in the midregion between existing joints where local tensile stress is highest. High remote tensile stresses may develop due to differential horizontal contraction among adjacent stratigraphic beds upon uplift and erosion.

INTRODUCTION

BEDDED sedimentary rocks often contain orthogonal joint sets consisting of an early systematic set and non-systematic joints extending across intervals between the systematic set. These latter joints are called cross joints (Hodgson 1961, Hancock 1985) and are not to be confused with systematic joints roughly perpendicular to fold axes some authors (e.g. Badgley 1965, Helgeson & Aydin 1991) call cross joints. Like systematic regional joints, cross joints are often regularly spaced, a phenomenon explained in detail in this paper. Joint spacing depends upon mechanical layering which commonly develops as a consequence of change in lithology.

A lithology-controlled mechanical layer is a unit of rock that behaves homogeneously in response to an applied stress and whose boundaries are located where changes in lithology mark contrasts in mechanical properties. For example, the two limestone beds in Fig. 1(a) are each considered mechanical layers because they do not exhibit lateral variations in mechanical behavior, as indicated by uniformly developed joints which consistently extend across the entire bed height (the 'jointed layer' of Pollard & Segall 1987). The limestone beds are bounded above and below by beds of unfractured mudstone. The contact between these beds acts as a mechanical layer boundary, and the distance between the two mechanical layer boundaries (i.e. the top and base of the limestone) constitutes a mechanical layer thickness. Often a mechanical layer thickness can be defined by the height of the joints contained within a bed.

Joint terminations in sedimentary rocks fall into two main categories, joints that terminate at random locations within a vertical section of rock mass, and those that terminate consistently at mechanical layer boundaries. The former joints are commonly observed in units of relatively homogeneous composition such as granites and massive thick-bedded carbonates where the distance between mechanical boundaries is substantially larger than joint height. The latter are found in well-stratified sections where adjacent layers have different mechanical properties, such as thin to medium interbedded limestones and shales. Stress discontinuities arising from contrasts in mechanical properties at lithologic contacts act as a barrier to joint propagation and thus confine joints to specific layers (Fig. 1a).

Joint spacing is directly proportional to lithology-controlled mechanical layer thickness in cases where joints are confined to specific lithologic beds (e.g. Price 1966, McQuillan 1973, Ladeira & Price 1981, Huang & Angelier 1989, Narr & Suppe 1991). This relationship is shown schematically in Fig. 1(a) where the limestone bed with the small mechanical layer thickness contains more closely spaced joints than the thick limestone bed. On plots of mechanical layer thickness vs joint spacing the slope of the best-fit line is referred to as the fracture spacing index (FSI) which is the ratio of mechanical layer thickness to median joint spacing (Narr 1991). The FSI is calculated in order to normalize fracture spacing among beds of different thickness and thereby evaluate fracture density. Median spacing is used because a non-normal joint spacing distribution is commonly observed. Ladeira & Price (1981) suggest that FSI is a function of lithology, whereas Narr (1991) reports a single FSI for all fractured Monterey lithologies.

This study tests the hypothesis that pre-existing systematic joints act as mechanical layer boundaries in the same manner as bedding planes, thereby controlling the spacing and length of a later set of joints. In this latter case a mechanical layer boundary is created by the free surface marking the joint plane rather than a lithologic contact which may be welded. For this reason the term *layer* is used instead of *bed* to avoid stratigraphic implications. The distance between adjacent pre-existing sys-

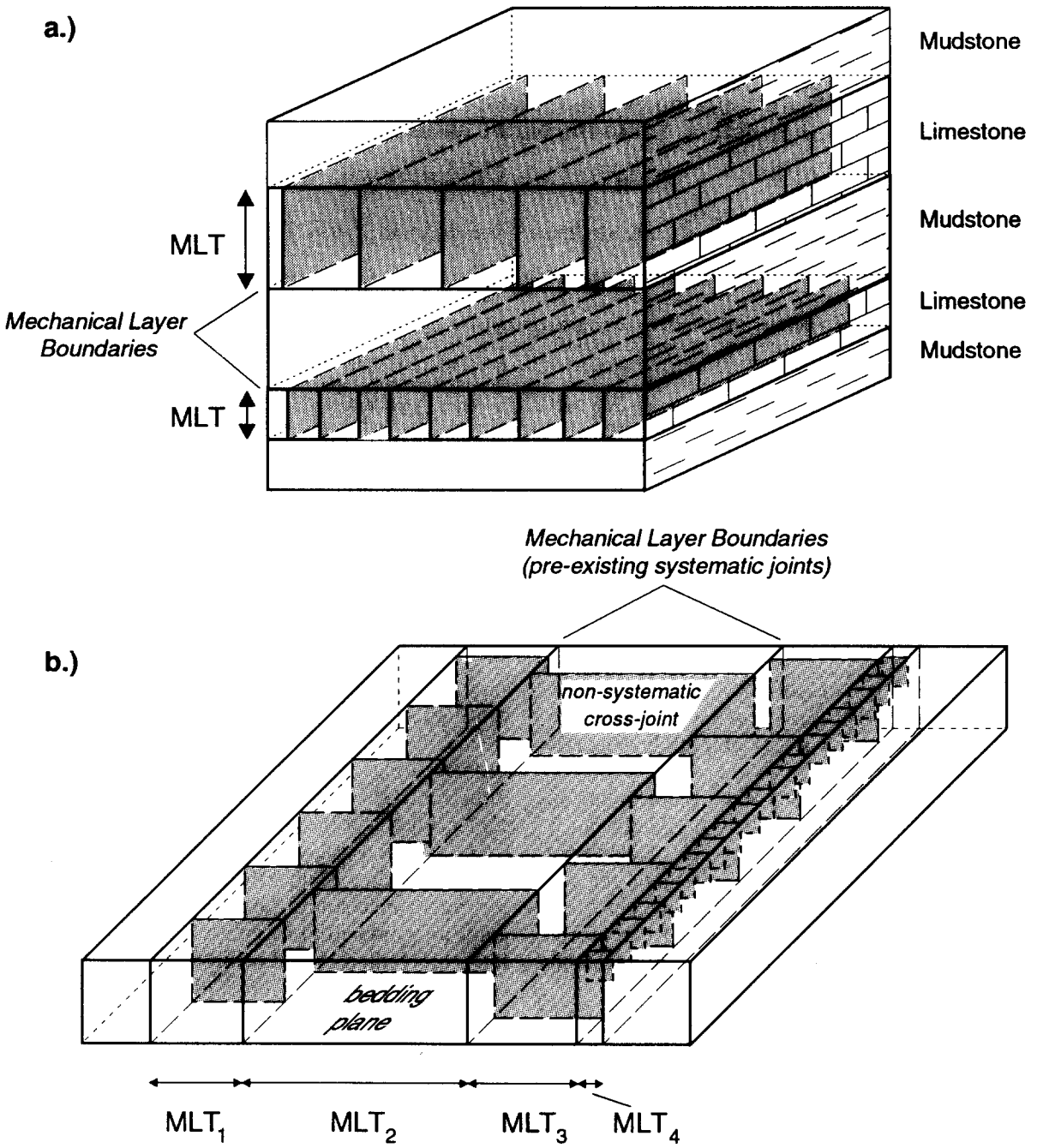

Fig. 1. Illustration of joints confined to mechanical layers. (a) Mechanical layer boundaries defined by lithologic contacts (lithology-controlled); (b) Mechanical layer boundaries defined by pre-existing joints (joint-controlled). Note that joint spacing is proportional to mechanical layer thickness (MLT) in both cases.

tematic joints represents a mechanical layer thickness and is therefore directly proportional to the spacing of the interconnecting cross joints which are often non-systematic (Fig. 1b). A linear relationship similar to the one reported for lithologically-controlled mechanical units should be observed between the spacing of pre-existing joints and the spacing of later connecting joints. From joint spacings, crack termination geometry, and a fracture mechanics model, it is possible to estimate the magnitude of principal horizontal tensile stress at the time of cross joint propagation.

FIELD OBSERVATIONS

Outcrops of the clayey-siliceous member of the Miocene Monterey Formation (Isaacs *et al.* 1983) at Alegria and Gaviota Beaches were investigated in order to test the hypothesis that systematic joints can act as mechanical layer boundaries. Alegria and Gaviota are located along the Santa Barbara Channel on the southern flank of the Santa Ynez Range (Fig. 2). The Monterey Formation is in the opal C-T phase of silica diagenesis at these two sites. West of Alegria Canyon the Monterey Forma-

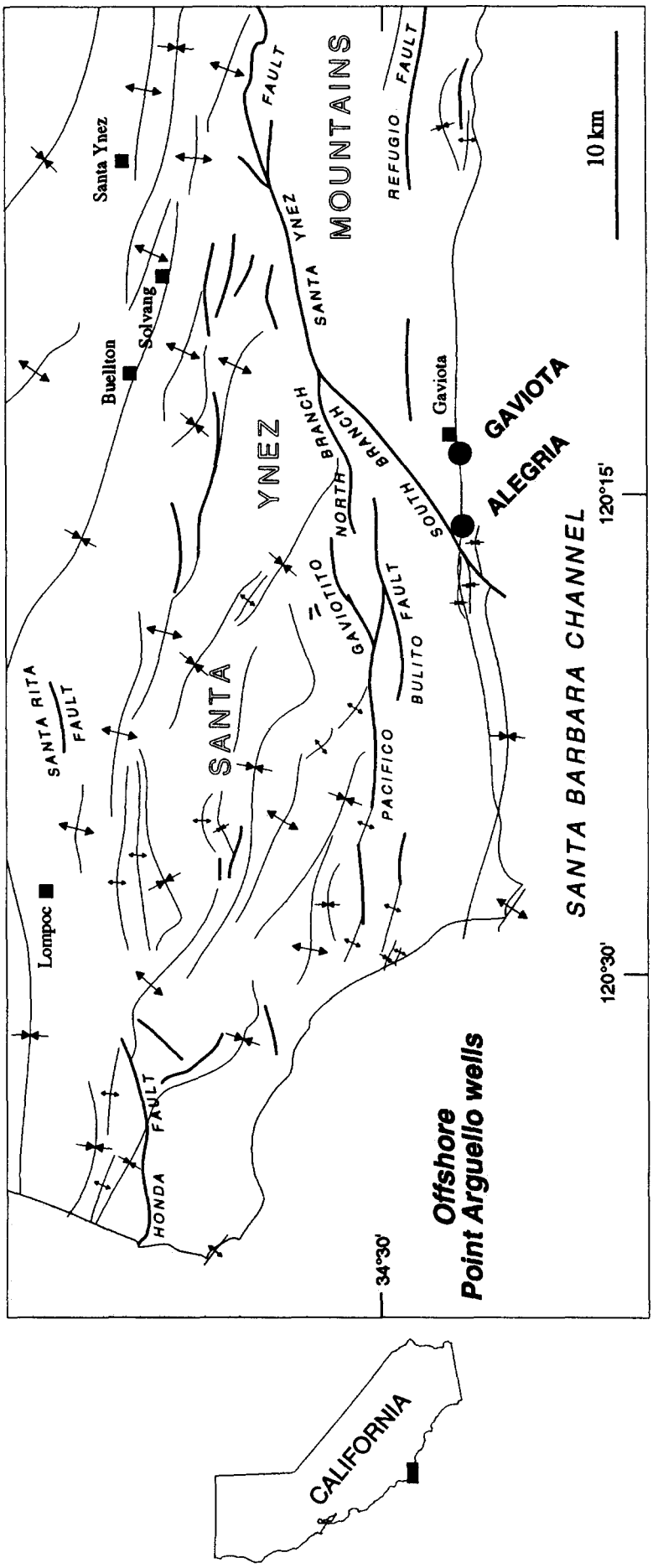

Fig. 2. Structural map of the western Santa Ynez Mountains, California, U.S.A. Adapted from Dibblee (1950, 1988a, b).

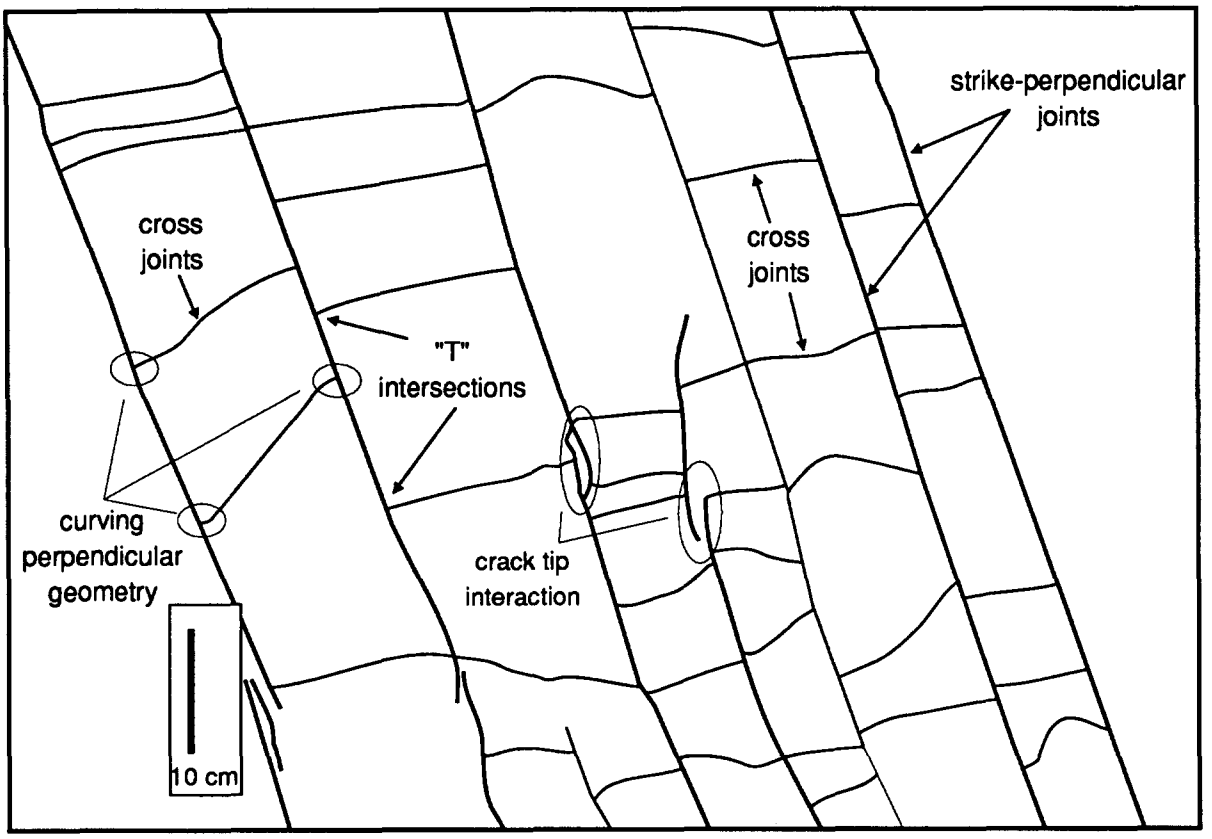

Fig. 3. Sketch of bedding plane surface at Alegria Station A.

tion terminates against the South Branch of the Santa Ynez Fault.

Joints and veins observed along coastal Monterey outcrops fall into three main orientations: strike-perpendicular, strike-parallel and bedding-parallel. Strike-perpendicular joints are oriented perpendicular to strike and normal to bedding, and are commonly referred to as 'cross-fold' joints (e.g. Hancock & Engelder 1989, Srivastava & Engelder 1990). In order to avoid confusion with non-systematic cross joints, the term strike-perpendicular will be used in place of 'cross-fold' to identify these joints. Strike-perpendicular joints and veins are typically the most dominant fractures found in the Monterey Formation both in the Santa Maria Basin north of the Santa Ynez Range and along the Santa Barbara coastline.

Description of joints

A total of five bedding plane surfaces in the clayey-siliceous member were selected for analysis, three at Gaviota and two at Alegria. The bedding plane surfaces strike approximately E–W and dip between 37° and 54° to the south. The systematic strike-perpendicular joints are vertical in outcrop, perpendicular to bedding strike and normal to the bedding plane surface. Non-systematic cross joints intersect the systematic joints at right angles and are oriented parallel to bedding strike and normal to the bedding plane surface. A sketch of a bedding plane surface at Alegria Station A displays many of the features of joints encountered during this study (Fig. 3). Stereonets of joint orientation data from Gaviota and Alegria show that angular relationships between joint sets and bedding are consistent at both localities (Fig. 4).

Systematic strike-perpendicular joints are extremely planar and very consistent in orientation, forming a tight cluster of points on the stereonets. Their traces on bedding plane surfaces span relatively long distances, with individual segments ranging in length from approximately 200 to 500 cm. Tips of the strike-perpendicular joints terminate within the host rock rather than against other joint surfaces, and in some cases curving tips suggest interaction of strike-perpendicular joints during propagation. In all cases the systematic strike-perpendicular joints are the oldest set of joints in the outcrop.

In contrast to strike-perpendicular joints, the non-systematic cross joints exhibit non-planar surfaces and irregular, curved traces on bedding plane surfaces. They are less consistent in orientation than strike-perpendicular joints and hence display more scatter on the stereonets. Cross joint lengths are controlled by the distance between systematic strike-perpendicular joints, and typically range in length from 1.5 to 45 cm. Cross joints always abut against pre-existing strike-perpendicular joints forming T-intersections, creating an H-shaped pattern (Hancock 1985) on the bedding plane surface. Crack tip interactions between cross joints are rarely observed, and cross-cutting relationships indicate cross joints are always the youngest set of joints.

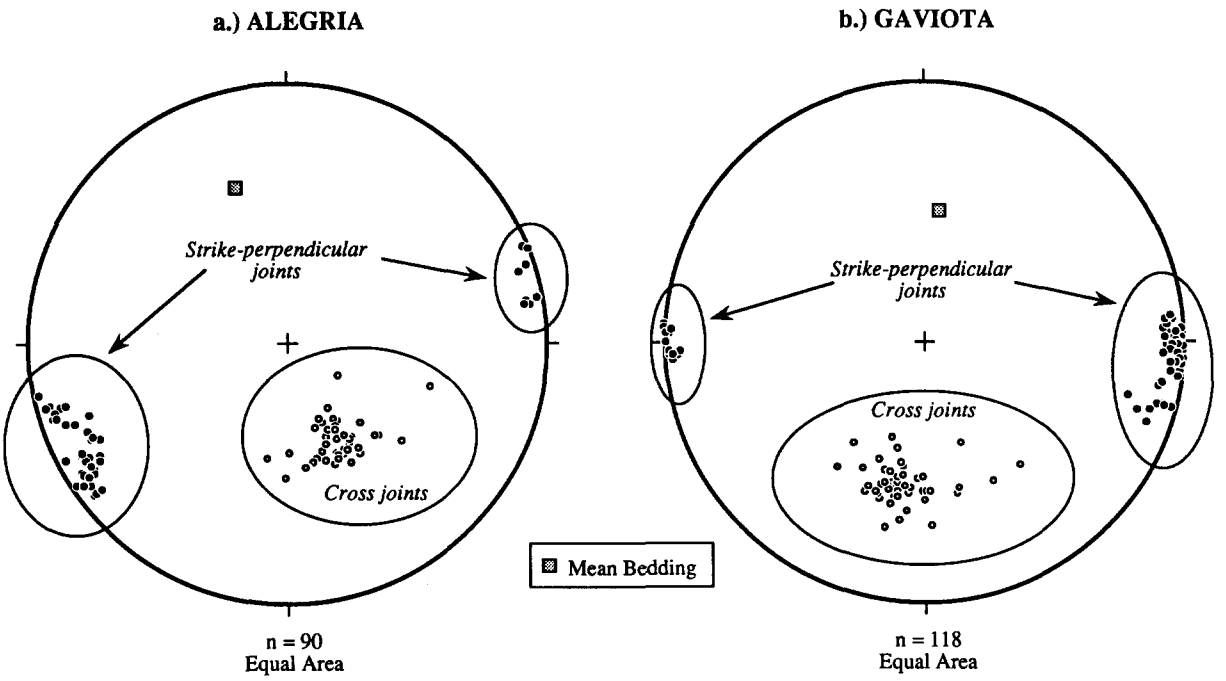

Fig. 4. Stereonets of joint data measured on bedding plane surfaces at (a) Alegria and (b) Gaviota.

Joint spacing vs mechanical layer thickness

Joint-controlled mechanical layer thickness was determined by measuring the spacing between adjacent pairs of systematic strike-perpendicular joints. In some cases this distance varied slightly along the length of the joint pairs, and thus an average mechanical layer thickness was calculated from a number of measurements. Thirty-four joint-controlled mechanical layers, or pairs of strike-perpendicular joints, were measured at the five stations with thicknesses ranging from 1.4 to 94.0 cm. The spacing of non-systematic cross joints between each individual pair of systematic joints was measured, and the median cross joint spacing was plotted vs mean mechanical layer thickness for each pair (i.e. spacing between systematic joints).

Plots of cross joint spacing vs joint-controlled mechanical layer thickness are presented in Figs. 5(a) & (b) and spacing data collected for this study are summarized in the Appendix. There is a strong linear relationship between the spacing of non-systematic cross joints and the distance between adjacent pairs of strike-perpendicular joints within which they are contained. The slope of the best-fit line through the origin, calculated with cross joint spacing as the dependent variable, is the fracture spacing index (FSI). The strong degree of linearity is reflected in the high correlation coefficients.

The linear relationships displayed in Figs. 5(a) & (b) indicate that pre-existing joints can act as mechanical layer boundaries, and their spacing reflects a mechanical layer thickness. Moreover, the FSI values for Alegria and Gaviota cross joints are nearly identical at 1.23 and 1.26, respectively, implying a consistent mechanical behavior from one locality to the next. The fracture spacing index for the combined data set from Alegria and Gaviota is 1.26 (Fig. 6). The FSI values for non-systematic cross joints determined in this study are similar to results from systematic joints in the Monterey Formation in the Santa Maria Basin (Narr 1991) and along the Santa Barbara Channel where lithologic contacts define mechanical layer boundaries (Table 1). They vary considerably from FSI values measured in other geologic provinces. One suggestion is that during uplift and erosion strata in the Monterey Formation become saturated with joints at a fracture spacing index of approximately 1.29 (Narr & Suppe 1991). When this fracture density is reached extensional strain is accommodated by opening existing joints rather than propagating new joints.

Cross joint spacing distribution

A number of statistical functions describe the distribution of fracture spacing in rock masses. Fracture spacing for all discontinuities intersecting a given scanline is expressed by a negative exponential distribution (Priest & Hudson 1976). However, this survey does not differentiate between fracture sets, and hence this result can be applied only to general bulk fracture analyses. Huang & Angelier (1989) reported that spacing of an individual joint set follows a gamma distribution, while Narr & Suppe (1991) concluded that strike-perpendicular joint spacing in the Monterey Formation follows a log-normal distribution.

Spacing values of cross joints within a given systematic pair were divided by the median cross joint spacing value according to the method of Narr & Suppe (1991), and then all of the normalized data were combined into a single histogram representing 710 cross joint spacing measurements (Fig. 7). Graphs of normal, log-normal and gamma probability density functions calculated using statistical parameters computed from the cross

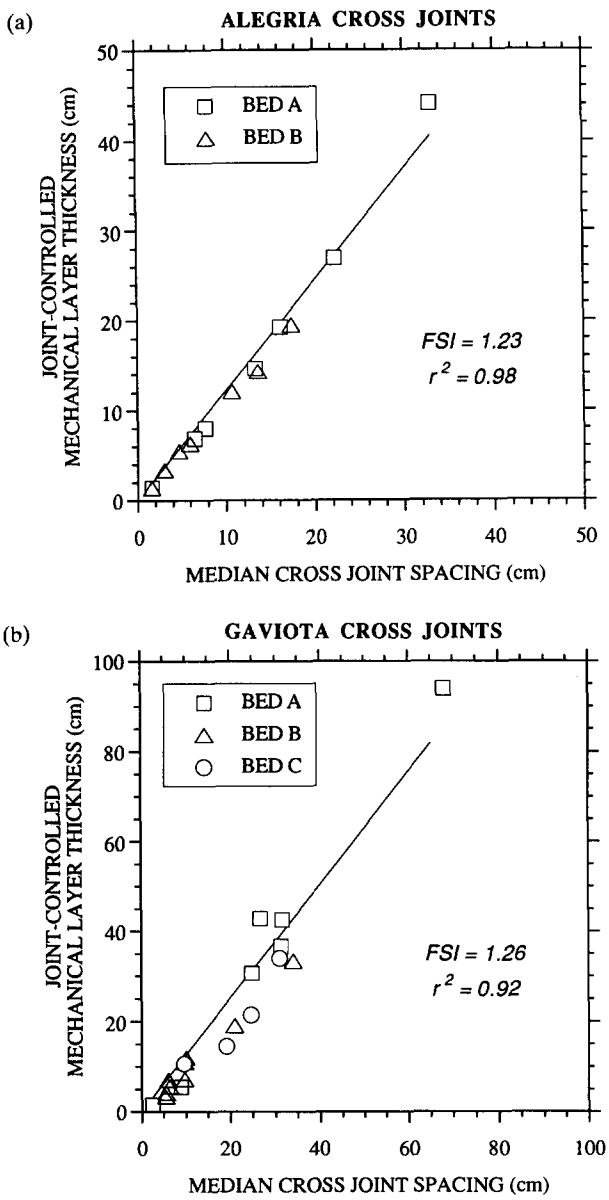

Fig. 5. Plots of joint-controlled mechanical layer thickness vs cross joint spacing for beds at (a) Alegria and (b) Gaviota. The slope of the best-fit line computed with spacing as the dependent variable is the fracture spacing index (FSI).

joint spacing data set are presented with the histogram. The chi-square criterion rejects the hypothesis that the data set belongs to either a normal or log-normal distribution with 99% confidence, though at a confidence level of 95% the chi-square test does not reject the

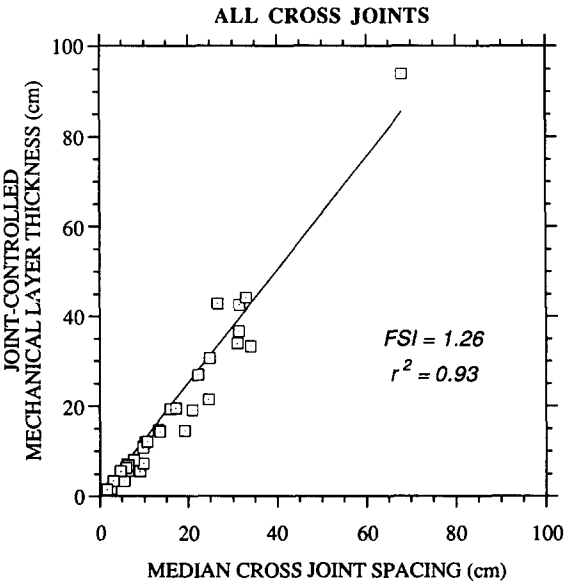

Fig. 6. Combined plot of joint-controlled mechanical layer thickness vs cross joint spacing for all data from Alegria and Gaviota.

hypothesis that the data set follows the gamma function. Therefore, while normal and log-normal distributions may be ruled out, it remains possible that cross joint spacing in the Monterey Formation is distributed according to the gamma function.

STRESS VALUES NECESSARY FOR CROSS JOINT PROPAGATION

Stress ratios from joint termination geometry

A stress ratio estimate at the time of cross joint propagation can be inferred from joint termination geometry. The chronological relationship between pre-existing strike-perpendicular joints and later cross joints along the Santa Barbara Channel is analogous to the joint sets described by Dyer (1988) in Arches National Park, Utah. Dyer (1988) investigated the propagation paths of younger joints as they approach a set of pre-existing systematic joints. The orientation of regional maximum horizontal compressive stress rotated between the two fracturing episodes so that the younger joints, which initiate in the midregion between the older joints, initially are oriented 30° away from the earlier set. Two types of interaction are observed, a curving parallel

Table 1. Fracture spacing index (FSI)

Formation	Locality	Joint type	FSI
Monterey Fm	Algeria	Cross joints (JC)	1.23
Monterey Fm	Gaviota	Cross joints (JC)	1.26
Monterey Fm	Algeria and Gaviota	Cross joints (JC)	1.26
Monterey Fm	Santa Maria Basin	Strike perpendicular and parallel (LC)*	1.29
Monterey Fm	Santa Barbara Channel	Strike perpendicular (LC)	1.32
Brallier Fm	Huntingdon, Pennsylvania	Strike perpendicular (LC)†	1.79
Ithaca Fm	Watkins Glen, New York	Strike perpendicular (LC)†	0.68

JC = joint-controlled mechanical layers; LC = lithology-controlled mechanical layers.
*Narr & Suppe (1991).
†Engelder & Gross (unpublished data).

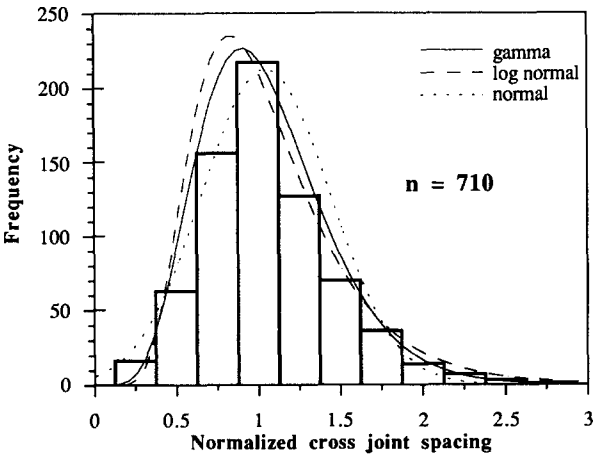

Fig. 7. Histogram of normalized cross joint spacing. Refer to text for details.

geometry where late joints parallel pre-existing joints upon approach, and a curving perpendicular geometry where late joints curve toward early joints and intersect them at approximately right angles. Dyer (1988) concluded that the pre-existing joints were open cracks (free surfaces) and subject to a net far field tensile stress. In the case of curving perpendicular geometry both the resolved stress normal and parallel to the pre-existing joint are tensile and $-\frac{1}{3} < \sigma^r_H/\sigma^r_h < 1$, where σ^r_H is the maximum horizontal principal stress and σ^r_h is the least horizontal principal stress.

Though many of the cross joints at Alegria and Gaviota are initially oriented orthogonal to the strike-perpendicular joint set, there are a number of cross joints that initiate at angles less then 90°. In all cases cross joints approach pre-existing joints with a curving perpendicular geometry (Fig. 3). In order to satisfy Dyer's analytical solution a net far field tensile stress is required both normal and parallel to the pre-existing strike-perpendicular joints. Such conditions are likely to exist near the Earth's surface as the Monterey Formation is uplifted and eroded, and less likely to occur at depth, especially in a region of compressional folding such as the western Transverse Ranges. It therefore appears that the ratio of maximum stress to minimum stress in the plane parallel to bedding is between $-\frac{1}{3}$ and 1.

Joint spacing models

A number of theoretical models attempt to explain joint spacing (Lachenbruch 1961, Price 1966, Hobbs 1967, Pollard & Segall 1987). In an effort to describe depth and spacing of tension cracks which propagate downward from a stress free surface (e.g. contraction cracks in ice, mud and extrusive rocks), Lachenbruch (1961) developed a model which solves for stress perturbations both normal and parallel to a joint surface. Because cross joint termination geometry within the Monterey Formation requires that cross joints initiate within the medium and propagate outward toward the free surface, the Lachenbruch model does not apply. Hobbs (1967) developed a model for joint spacing in which a jointed layer with a larger Young's modulus is situated between two unjointed layers with a smaller Young's modulus. The Hobbs model requires changes in elastic properties across mechanical layer boundaries as well as the development of shear stresses along boundaries of neighboring layers. Though appropriate for lithology-controlled mechanical layers, the Hobbs model does not apply to joint-controlled mechanical layers because on a bedding plane surface there are no changes in elastic properties across joint-controlled mechanical layer boundaries, and shear stresses cannot be transmitted across free surfaces.

One appropriate model for cross joint spacing was developed by Pollard & Segall (1987), who present a theoretical solution for joint spacing assuming an infinite elastic medium and constant elastic properties for all layers. They demonstrate that the stress field is perturbed in the vicinity of a newly formed joint, and conclude that this stress perturbation is precisely the factor controlling joint spacing. The magnitude of local stress normal to the joint surface (σ_{11}) at a distance away from the joint is a function of distance from the joint (x_1) and mechanical layer thickness (T):

$$\sigma_{11}\left(\frac{x_1}{T}, x_2 = 0\right) = \sigma^r_{11} 8 \left|\frac{x_1}{T}\right|^3 \left[4\left(\frac{x_1}{T}\right)^2 + 1\right]^{-3/2}. \quad (1)$$

Tensile stress normal to the joint surface is zero, and increases as a percentage of the remote tensile stress (σ^r_{11}) with increasing distance away from the joint along the x_1 axis. In effect, the process of joint propagation creates a stress reduction shadow around the newly formed joint, and the amount of stress reduction at a given distance from the joint is directly related to the joint height, which in this case defines the mechanical layer thickness. Thus, local tensile stress rises to 30% of the remote tensile stress at a distance $0.45(x_1/T)$, 50% at $0.65(x_1/T)$, 70% at $0.97(x_1/T)$, and 90% at $1.85(x_1/T)$. The ratio of local tensile stress to remote stress in equation (1) is plotted in Fig. 8(a) and the stress reduction in the vicinity of a newly formed joint based on this analysis is shown schematically in Fig. 8(b).

Crack driving stress for an individual flaw

Fracture mechanics approaches the process of joint propagation through the analysis of stress intensity near the crack tip. The magnitude of the crack tip stress field in a homogeneous linear elastic medium is defined by the stress intensity factor (K) which is a function of applied load, crack geometry and crack length (Atkinson 1987):

$$K = -Y\sigma^r\sqrt{\pi c}. \quad (2)$$

Remote tensile stress is σ^r, c is the crack half-length, and Y is a numerical modification factor related to crack geometry, loading conditions and edge effects. Mode I crack extension occurs when the critical stress intensity factor K_{Ic} is reached. Equation (2) means that for larger initial crack lengths a lower remote tensile stress is

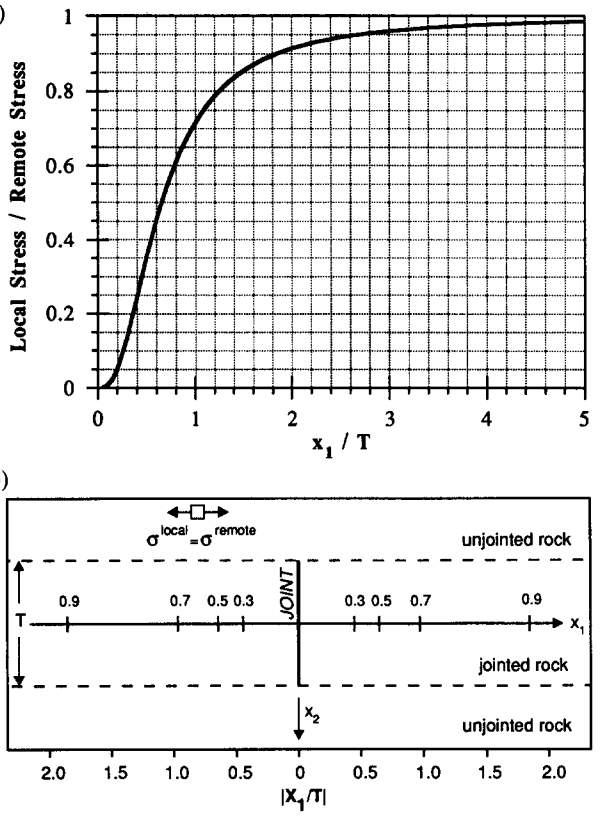

Fig. 8. Pollard & Segall (1987) model for stress reduction in the vicinity of a newly formed joint. (a) Plot of local stress/remote stress ratio as a function of distance from joint (x_1) and bed thickness (T) (equation 1). Note that local stress values approach the remote stress with increasing distance. (b) Schematic diagram of Pollard & Segall model showing stress reduction ratio in a jointed layer.

required for fracture propagation. Geologic sign convention is used throughout this paper, where tensile stress is negative and compressive stress is positive.

Inspection of samples from stations at Alegria and Gaviota reveals abundant microfossils 1 mm in diameter. Though less numerous, fossils and discontinuities with lengths in the range of 0.5 cm are common, whereas 1.0 cm discontinuities are present but rare. These observations are consistent with the negative exponential distribution reported for macroscopic joint lengths (e.g. Segall & Pollard 1983). Large flaws are expected to act as stress concentrators from which cross joints propagate, therefore remote stresses are calculated using 0.5 cm and 1.0 cm as initial flaw sizes. An estimate of 1.8 MPa $m^{1/2}$ for K_{Ic} was selected (Senseny & Pfeifle 1984, Atkinson & Meredith 1987), along with a modification factor of $Y=1.0$ for elliptical-shaped cracks in an infinite elastic medium. Inputting these parameters into equation (2), the remote tensile stress required for joint propagation is -20.3 MPa for an initial flaw size of 0.5 cm (i.e. $c = 0.25$ cm) and -14.4 MPa for an initial flaw size of 1.0 cm (i.e. $c = 0.5$ cm). This calculation assumes joint initiation in an infinite elastic medium, whereas in reality the mechanical layer boundaries created by pre-existing strike-perpendicular joints act as free surfaces resulting in a semi-infinite medium. The validity of assuming an infinite elastic medium therefore depends upon the ratio of initial flaw size to mechanical layer thickness. This assumption is reasonable for most Monterey cross joint calculations.

Assumptions for cross joint model

Two possibilities exist for the relative timing of cross joint propagation: either they all propagate simultaneously or a sequential infilling occurs whereby younger joints initiate in the region between pre-existing cross joints. In the former case stress shadows would not be a factor since all joints propagate at the same time. In order for Monterey cross joints to propagate simultaneously, initial flaws of a given size must be distributed in a manner such that their spacing within a given joint-controlled mechanical layer reflects a fracture spacing index of 1.3. Given the variability of joint-controlled mechanical layer thicknesses at Gaviota Station B (3.35–33.40 cm), flaws in one portion of the bedding plane surface would have a required spacing of 2.5 cm, whereas flaws would be spaced 25.7 cm apart in another section. Flaws are primary sedimentary features such as fossils and sedimentary structures, and their distribution on a specific bedding plane horizon should be relatively uniform. Therefore, it is not likely that Monterey cross joints propagated simultaneously.

A more realistic scenario is the sequential infilling of joints, a process influenced by the reduction of remote stress in the vicinity of a newly-formed joint. Sequential fracture infilling is commonly observed in tensile loading of layered ceramics (Garrett & Bailey 1977) and elastically deformed plaster (Ghosh 1988). Crack driving stresses for sequential infilling are based on the Pollard & Segall (1987) model of stress reduction in the vicinity of a newly formed joint (Figs. 8a & b). A number of assumptions are required in order to proceed with the analysis of sequential joint propagation.

(1) Initial joint propagation from a pre-existing flaw occurs in an infinite elastic medium, and is not influenced by free surfaces at mechanical layer boundaries; cross joints predominantly propagate from initial flaws 0.5 cm in diameter as suggested by outcrop observations.

(2) Cross joints propagate when local stresses reach 90% of the remote crack driving stress. A ratio of $(0.9)\sigma^r$ corresponds to a distance of $(1.85)(x_1/T)$ from the joint surface. Beyond this distance the slope of the Pollard & Segall curve is less than 0.1, and a large increase in distance results in only a small change in percentage of remote stress (Fig. 8a).

(3) Reduction in stress at a point influenced by two adjacent joints is calculated using linear scaling, a common procedure in elasticity solutions. For example, if the presence of one joint reduces the local stress to $0.7(\sigma^r)$ at a given point, and a second joint creates an $0.8(\sigma^r)$ reduction, then the local stress is found by superposition: $(0.7)(0.8)(\sigma^r)$ or $0.56(\sigma^r)$.

(4) Since the stress across a joint surface equals zero, the reduction in stress at any given point is influenced only by the two adjacent joints, regardless of joint spacing.

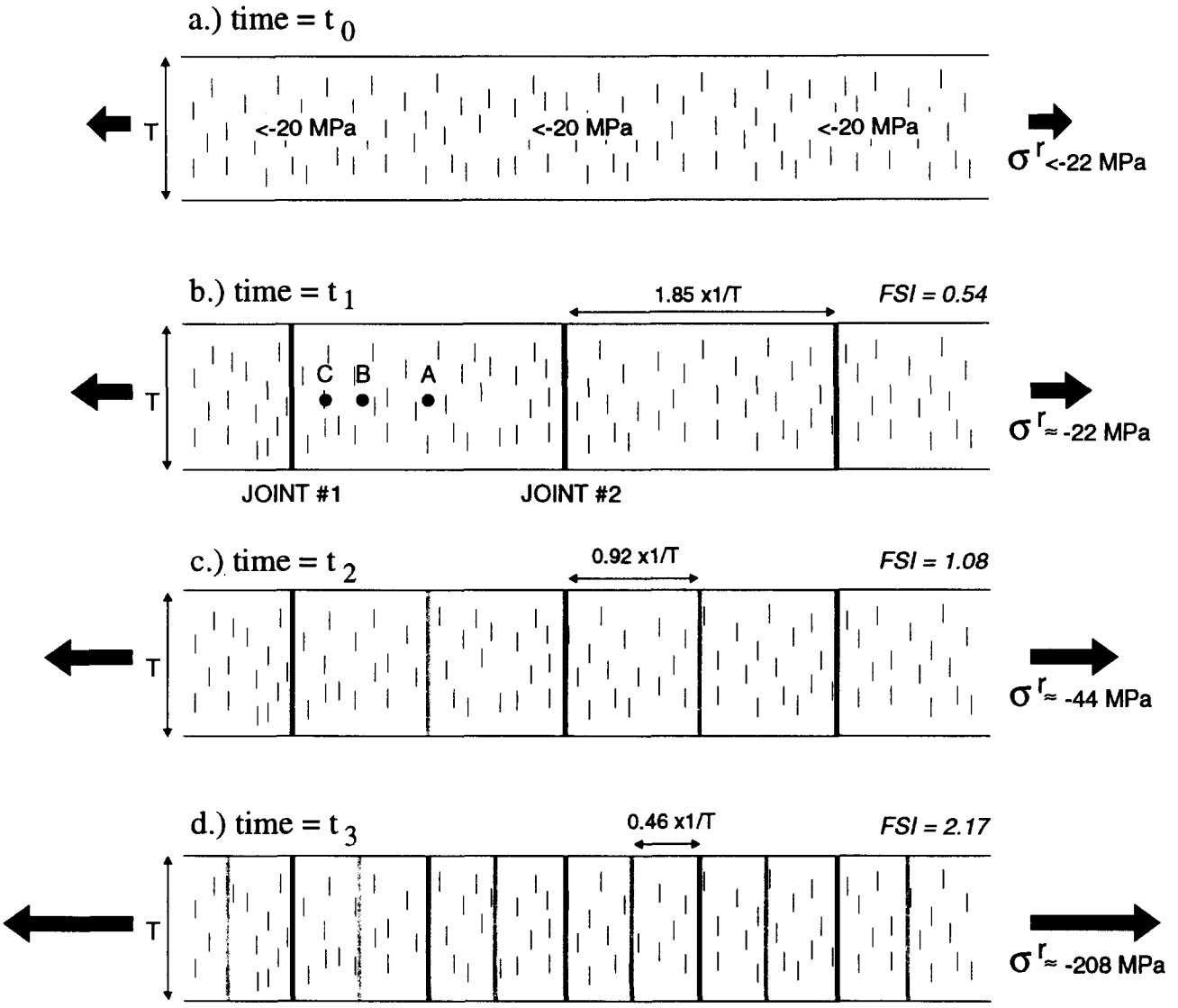

Fig. 9. General model for sequential joint infilling in a mechanical layer containing abundant 0.5 cm flaws. Refer to text for more details.

(5) Joints do not initiate in the vicinity of mechanical layer boundaries. As discussed earlier, the curving perpendicular geometry of Monterey cross joints implies that they originate in the midregion of mechanical layers.

(6) Joint propagation occurs instantaneously.

(7) Remote stress is transmitted to the jointed layer through the welded contacts of adjacent stratigraphic horizons.

General sequential infilling model

For the general model, flaws 0.5 cm in length are distributed throughout the layer with an initial spacing much closer than the final cross joint spacing. Initially tensile stress at the flaw tips is below the value for crack driving stress, and joints do not propagate (Fig. 9a, time = t_0). Remote tensile stress increases, and local stress at the flaw tips approaches −20 MPa, the approximate stress required to initiate a joint from a 0.5 cm flaw (Fig. 9b, time = t_1). Since the local stress at joint propagation is assumed to represent 90% of the remote tensile stress, the remote tensile stress is approximately −22 MPa. Once these stress conditions are reached a first set of cross joints forms. During this stage joints do not propagate all at once due to variations in initial flaw size. Hence, joint initiation is influenced by stress shadows of other joints within the layer, and the minimum joint spacing possible during this episode is $1.85(x_1/T)$, which corresponds to a fracture spacing index of 0.54. This is because at distances less than $1.85(x_1/T)$ the local tensile stress is less than −20 MPa. Therefore, assuming a high density of 0.5 cm flaws, the first generation of cross joints propagates at a remote stress of −22 MPa resulting in a fracture spacing index of 0.54.

In this model the next generation of cross joints will propagate only after an appreciable increase in remote tensile stress. At any point along the x_1 axis the local tensile stress is now reduced by the presence of the two adjacent joints. For example, point A at the midpoint between Joints 1 and 2 is located a distance of $0.92(x_1/T)$ from either joint (Fig. 9b). Both joints have the effect of

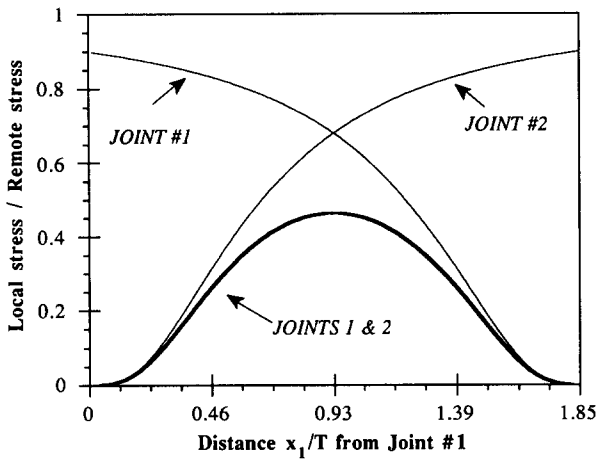

Fig. 10. Plot of stress reduction as a ratio of local stress/remote stress along the x_1 axis between Joints 1 and 2 in Fig. 9(b). Thin curves are the stress reductions caused by the individual joints whereas the bold curve represents the combined stress reduction effect.

reducing the local stress by a factor of 0.68 (σ^r), so that at point A the local stress is reduced by a total of (0.68)(0.68)(σ^r) or 0.46(σ^r). A plot of local stress as a function of remote stress for any point lying along the x_1 axis situated between two joints spaced 1.85(x_1/T) apart is shown in Fig. 10. Note the highest value of stress is located at the midpoint between the two joints, and it is at this point along the x_1 axis where the crack driving stress will first be reached. In order for the crack driving stress to reach −20 MPa at point A, the remote tensile stress must increase to (−20 MPa)/(0.46) or −43.5 MPa. Once this value is reached at time $t = t_2$ a second generation of cross joints will propagate, initiating in the midregion between adjacent first generation joints (Fig. 9c). At this point the joint spacing is 0.92 (x_1/T) which corresponds to a fracture spacing index of 1.08.

Following the same procedure a third generation of cross joints will initiate when a remote tensile stress of −208 MPa is achieved. Resulting cross joint spacing is 0.46(x_1/T), which translates to a fracture spacing index of 2.17 (Fig. 9d). The fact that fracture spacing index values greater than 2.0 are rarely observed in jointed layers reflects the high stresses required for such configurations. While remote tensile stress increases with successive jointing events, local tensile stress within the jointed layer never exceeds the crack driving stress of approximately −20 MPa. Figure 11 is a plot of local tensile stress vs time for points A, B and C located along the x_1 axis of Fig. 9b. Joint propagation results in an immediate local stress drop followed by gradual stress increase until the next jointing event.

Stress model for Monterey cross joints

An attempt to reconstruct the stress history of Monterey cross joints based on theoretical considerations outlined above involves working backward through time. The observed fracture spacing index of 1.30 marks the final stage in the jointing process (i.e. time = t_f). At this point joint spacing relative to layer thickness is (x_1/T) = 0.77, and assuming a sequential infilling pro-

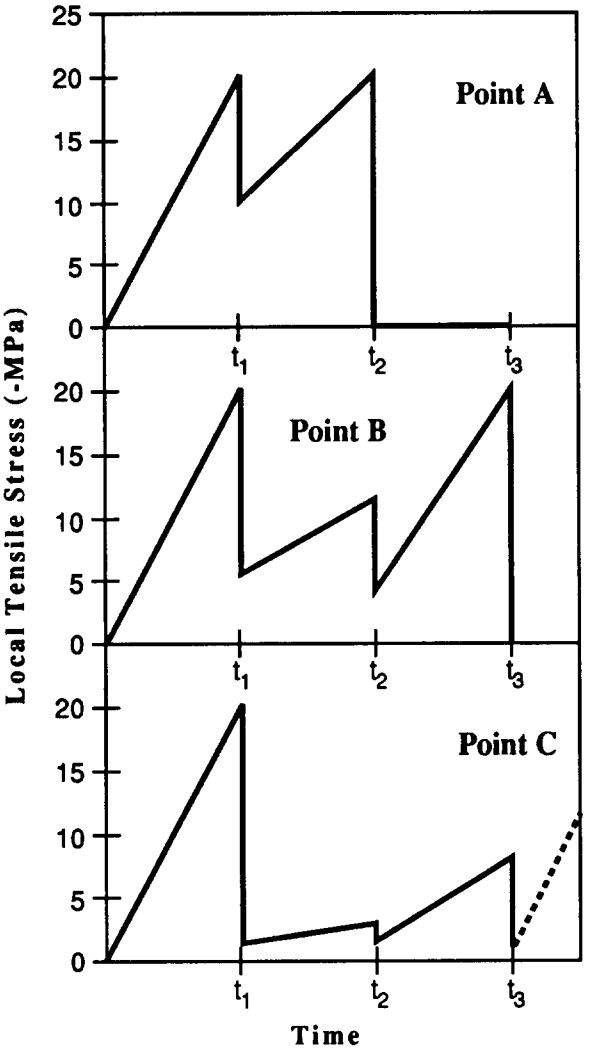

Fig. 11. Plots of local tensile stress vs time for points A, B and C in Fig. 9(b).

cess, the last joints to form initiated in the midregion at an equal distance of 0.77 (x_1/T) from adjacent pre-existing joints (Fig. 12a). Each pre-existing joint reduces the stress by a factor of 0.59 (σ^r) so that the local stress at the time of joint propagation (t_f) is $(0.59)^2(\sigma^r)$ or 0.35(σ^r). This corresponds to a remote tensile stress of (−20 MPa)/(0.35) or −57 MPa for the last generation of cross joints at time t_f, assuming a crack driving stress of −20 MPa.

Prior to the final fracturing event cross joints are spaced at intervals of 1.54 (x_1/T). In order to create this geometry, a stage of infilling occurs where cracks initiate from 0.5 cm flaws at a distance of 1.54(x_1/T) from adjacent pre-existing joints (time = t_{f-1}). Each pre-existing joint contributes a stress reduction of 0.86(σ^r) resulting in a local stress at the point of initiation equivalent to $(0.86)^2(\sigma^r)$ or 0.74 (σ^r) (Fig. 12b). Remote tensile stress during this stage of cross joint propagation is (−20 MPa)/(0.74) or −27 MPa.

Cross joint spacing prior to the t_{f-1} event is 3.08(x_1/T). This configuration could not have been created by a previous infilling event involving initiation from 0.5 cm flaws because a prior spacing of 6.16(x_1/T)

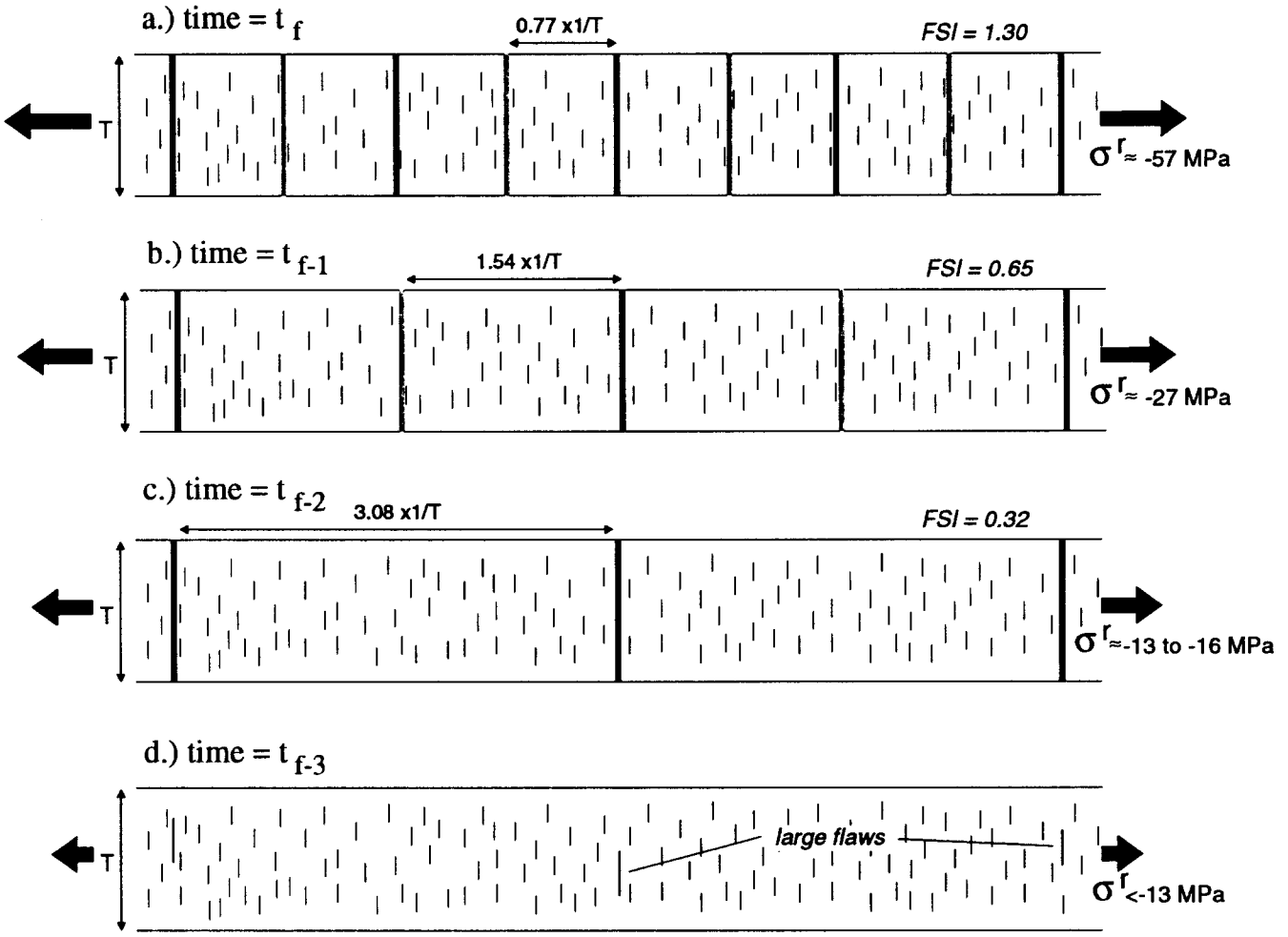

Fig. 12. Sequential infilling model for Monterey Formation cross joints. Refer to text for details.

would mean that 40% of the layer would have been subjected to local stresses in excess of 90% of the remote stress. Flaws 0.5 cm in length in these regions would have propagated since local stresses would have been greater than the required crack driving stress. An alternate scenario is that the first joints to form initiate from larger flaws which are widely spaced (Fig. 12d). These initial flaws may be in the size range of 1.0 cm and therefore would propagate at lower values of remote stress than the more abundant 0.5 cm flaws. Joint spacing during this initial phase of fracturing is not controlled by stress reduction shadows because the larger flaws are widely spaced relative to mechanical layer thickness. Later sequential infilling joints initiate from smaller 0.5 cm flaws under the influence of stress shadows.

Figure 13 summarizes the stress model for Monterey cross joint propagation. The first phase of fracturing occurs when joints initiate from a spectrum of large, widely spaced flaws ranging in size from 0.8 to 1.2 cm (time = t_{f-2}). Propagation occurs under remote stress conditions of −13 to −16 MPa and spacing of these early joints is approximately $3.08(x_1/T)$. Remote tensile stress increases with time to −27 MPa, at which point the crack driving stress for the more abundant 0.5 cm flaws is reached at the midpoint between the first set of cross joints. A second generation of cross joints then propagates from 0.5 cm flaws (time = t_{f-1}), resulting in a spacing of 1.54 (x_1/T). Each joint surface acts to reduce tensile stress in its vicinity, and the highest stress value along the x_1 axis is located at the midpoint between two joints. For a joint spacing of $1.54(x_1/T)$ the local stress at the midpoint is 35% of the remote tensile stress. Remote

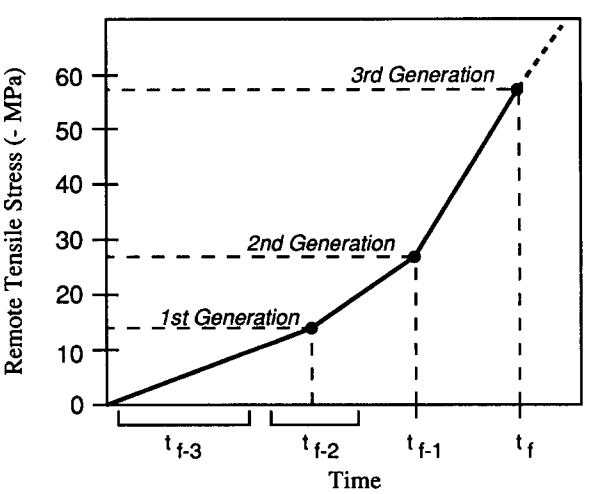

Fig. 13. Plot of remote tensile stress vs time for the sequential infilling model presented in Fig. 12 showing the three jointing events.

stress continues to increase, and at −57 MPa the crack driving stress for 0.5 cm flaws is once again reached at the midpoints, and a third generation of cross joints propagates (time = t_f). This is the final fracturing episode, creating a joint spacing of $0.77(x_1/T)$, or a fracture spacing index of 1.30. The remote tensile stress required for a fourth cross joint fracturing event is approximately −380 MPa, a geologically unreasonable value, which explains why a fourth jointing episode does not occur in this lithology. Though Narr & Suppe (1991) suggest that a fracture spacing index of 1.29 for systematic joints in the Monterey Formation reflects a saturation level, the model proposed in this study implies cross joint spacing is a function of the magnitude of remote tensile stress.

The model presented in this paper is based on a number of assumptions and is useful as a first-order approximation of the stress regime responsible for cross joint propagation. In reality, the fact that the distribution of cross joints is skewed indicates that sequential infilling does not occur precisely at midpoints. Although local stress is highest in the midregion between pre-existing joints (Fig. 10), there may not be a flaw of appropriate size exactly at that position. The likely case of randomly distributed initial flaws would result in a skewed rather than a normal spacing distribution (Narr & Suppe 1991), which in fact is observed among cross joints in the Monterey Formation (Fig. 7). Hence, values for remote tensile stress at the time of various jointing events reflect minimum stress values since joints are not always propagating in regions of maximum local tensile stress. Another simplifying assumption used in this model is that joint initiation is controlled by two populations of initial flaws, an abundant set of closely-spaced flaws 0.5 cm in length, and a set of less common 1.0 cm flaws which are widely spaced. In actuality a continuum of flaw sizes probably exists since flaw size is expected to follow a negative exponential distribution. Such a distribution predicts that small flaws will be more abundant than large flaws, which concurs with field observations in the Monterey Formation. Dividing critical flaw sizes into two populations provides the opportunity to estimate stress magnitudes during various stages of joint propagation, though an individual jointing event probably occurs over a range of stresses rather than at an exact critical value due to the spectrum of flaw sizes.

Constraints on remote maximum horizontal principal stress

Calculations of the remote tensile stress in the previous section correspond to the remote least horizontal principal stress (σ_h^r) at the various stages of fracturing. Constraints on the remote maximum horizontal principal stress (σ_H^r) can therefore be made based on Dyer's (1988) analysis. A curving perpendicular geometry of cross joints implies principal stress ratios of $-\frac{1}{3} < \sigma_H^r/\sigma_h^r < 1$. Estimates of the maximum and least horizontal principal stresses for Monterey cross joints during the three proposed fracturing events are listed in Table 2.

Table 2. Approximate values for minimum horizontal principal stress (σ_h^r) and maximum horizontal principal stress (σ_H^r) during stages of Monterey cross joint development

Jointing event	Time	σ_h^r (MPa)	σ_H^r (MPa)
First generation	t_{f-2}	−13 to −16	−16 to 4.7
Second generation	t_{f-1}	−27	−27 to 9
Third generation	t_f	−57	−57 to 19

The stress ratios of $-\frac{1}{3} < \sigma_H^r/\sigma_h^r < 1$ for curving perpendicular joints are valid for the specific case described by Dyer (1988) where the cross joints initiate at an angle of 30° away from the older joint set. Because pre-existing systematic joints are so closely spaced at Alegria and Gaviota, the initiation angle of the cross joints is impossible to determine. *In situ* stress measurements and earthquake focal mechanisms indicate that the maximum horizontal principal stress (S_H) is oriented NNE–SSW in the western Santa Barbara Channel region. Thus, if the cross joints indeed represent a late phase of deformation, they were subjected to a far field S_H oriented approximately 30° away from the systematic joint set during propagation. For this reason I selected the stress ratios $-\frac{1}{3} < \sigma_H^r/\sigma_h^r < 1$ to generate estimates of S_H in Table 2.

In general the driving stress for joint propagation can include both a remote tension and a fluid pressure within the joints (Segall & Pollard 1983). Thus remote stress can remain compressive if the fluid pressure is great enough. A combination of remote tension and internal fluid pressure as the driving mechanism for cross joint propagation will result in a much more complex derivation of stress history. In this scenario cross joint propagation occurs under conditions of effective tensile stress rather than absolute tensile stress, and an analysis of both internal fluid pressure and remote stress at each stage of jointing is required.

HOW CROSS JOINTS MIGHT FORM

The 'Poisson effect'

Non-systematic cross joints of the type described in this paper appear in less than 20% of the beds exposed along the Alegria and Gaviota coastlines, implying that tensile stresses necessary for cross joint propagation are local phenomena which are not uniformly distributed throughout the rock mass. One mechanism that may explain the origin of cross joints involves the relative expansion and contraction of neighboring stratigraphic layers. Consider a bed with a relatively high Poisson's ratio situated between two beds of relatively low Poisson's ratio (Fig. 14a). As the beds are brought to the surface upon uplift and erosion they will expand vertically as a result of overburden removal. Due to its higher Poisson's ratio the middle bed will tend to contract more on vertical expansion than its neighboring beds (Fig. 14b). Contraction, however, is prevented by the fact

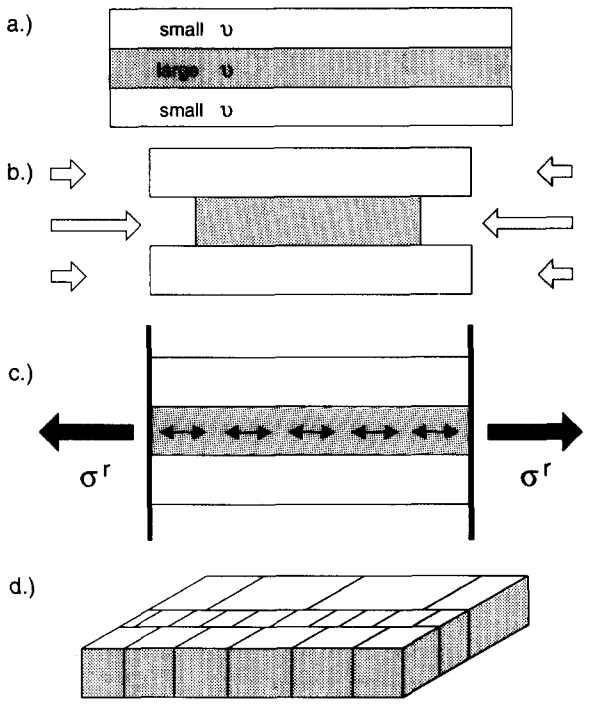

Fig. 14. Model for cross joint development in the Monterey Formation. (a) Beds at depth; (b) tendency for differential contraction due to variations in Poisson's ratio, ν; (c) tensile stresses develop in middle bed since layers are welded together; and (d) cross joints propagate in response to tensile stress.

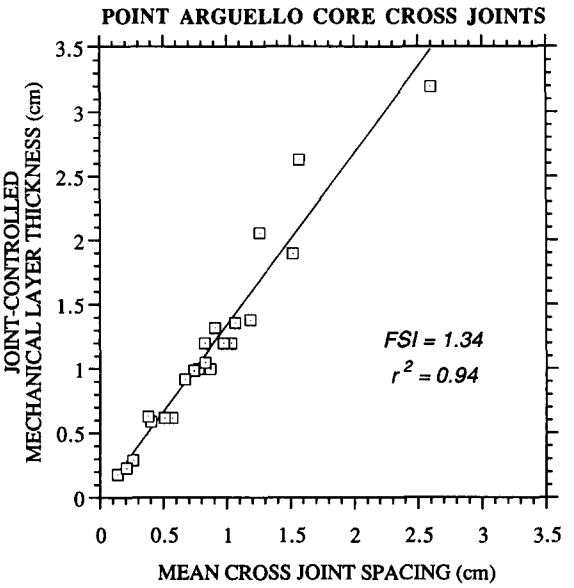

Fig. 15. Plot of joint-controlled mechanical layer thickness vs mean cross joint spacing in Monterey Formation core from four wells in the Point Arguello oil field, offshore California.

that beds are welded together along their boundaries. Therefore, a net tensile stress develops in the middle bed (Fig. 14c), resulting in the propagation of cross joints only in those layers where large contrasts in Poisson's ratios exist with neighboring beds (Fig. 14d). This mechanism for cross joint development is consistent with an increase in remote tensile stress with time (Fig. 13), and is not necessarily limited to uplift since it can occur during burial as overburden is added. The phenomenon of differential lateral expansion or contraction due to addition or removal of overburden is termed the 'Poisson effect'.

Jointing near the Earth's surface and in the subsurface

Exfoliation or sheet fractures (Gilbert 1904, Jahns 1943, Johnson 1970, Fleischman 1991) and neotectonic joints (Hancock & Engelder 1989, Gross & Engelder 1991) are examples of fractures believed to form at or near the Earth's surface in response to uplift and erosion. Sheet fractures tend to parallel the topographic surface and increase in spacing with increasing depth. Neotectonic joints are late formed vertical fractures aligned parallel to in situ maximum horizontal compressive stress. The least principal stress is vertical in the case of sheet fractures and horizontal for neotectonic joints. Though crack driving stresses for fluid driven joints propagating at depth have been estimated from hydraulic fracturing (e.g. Evans *et al.* 1989) and outcrop studies (e.g. Segall & Pollard 1983, Engelder & Lacazette 1990), the processes involved in near surface crack propagation remain enigmatic. Some cross joints in the Monterey Formation may have formed near the Earth's surface and therefore may contribute to the understanding of near surface fracturing processes.

The process of cross jointing is not restricted to the Earth's surface. Cross joints were observed in core from four wells in the offshore Point Arguello oil field (Fig. 2). These joints are present in thin bedded cherts and dolomites of the Monterey Formation at cored depths ranging from 2180 to 2870 m. The same relationship between joint-controlled mechanical layer thickness and cross joint spacing exists in the subsurface at Point Arguello, with a fracture spacing index of 1.34 (Fig. 15), a value similar to the fracture spacing index observed along the Santa Barbara Channel. Large differences in elastic properties within layered sedimentary rocks and high fluid pressures may lead to effective tensile stresses at depth, resulting in cross joint propagation.

Constraints on principal horizontal stresses

In a study of joints in the Mount Givens Granodiorite of the Sierra Nevada, Segall & Pollard (1983) calculate relative tensile stresses (remote stress plus internal fluid pressure) of approximately -1 to -40 MPa for crack propagation. Results from stress analysis of Monterey cross joints fall within the approximate range of -13 to -57 MPa. In experiments involving long, narrow rectangular plates undergoing uniaxial extension with the long axis initially aligned at 30° or 60° with the extension direction, Ghosh (1988) observed that extension fractures always propagate normal to the length of the plate. Likewise, Burg & Harris (1982) describe field examples of boudins and associated extension fractures which form angles of 45–90° to the maximum extension direction as determined from fiber growth. Therefore,

though constraints have been made on the magnitudes of σ_H and σ_h, the orientation of the principal horizontal stresses with respect to the joint sets is less certain.

Analogy with boudinage

Cross joint development is similar to certain boudinage processes. In fact, results from one of Ghosh's (1988) experiments with plaster of Paris yields a fracture pattern nearly identical to the bedding plane surfaces at Alegria and Gaviota. In this experiment Ghosh placed a lineated plate of plaster under axial symmetric extension. Fractures parallel to the lineation developed immediately. As the experiment continued a set of fractures subsequently formed perpendicular to the lineation. Careful examination of Ghosh's fig. 5(f) reveals that the younger fractures consistently abut against the pre-existing lineation-parallel fractures and the spacing between younger fractures is directly proportional to the distance between adjacent lineation-parallel fractures. This experiment is analogous to Monterey cross joints where pre-existing strike-perpendicular joints are represented by the lineation or lineation-parallel fractures, cross joints are the fractures which develop perpendicular to the lineation, and $\sigma_H/\sigma_h = 1$, one of the end members from Dyer's (1988) analysis. Furthermore, Ghosh (1988) observed that sequential midpoint fracturing occurs consistently in plates which have not undergone perceptible pre-fracture permanent deformation.

CONCLUSIONS

A set of pre-existing joints may act as mechanical layer boundaries during subsequent jointing events in much the same manner as lithologic contacts restrict joint propagation. The distance between adjacent strike-perpendicular joints exposed in bedding plane surfaces of the Monterey Formation constitutes a joint-controlled mechanical layer thickness within which a late forming series of non-systematic cross joints is contained. Spacing of cross joints is directly proportional to the distance between pre-existing strike-perpendicular joints, and joint termination geometry indicates that cross joints initiated in the midregion between strike-perpendicular joints.

The fracture spacing index, or ratio of joint-controlled mechanical layer thickness to joint spacing, is approximately 1.3 for cross joints observed in the Monterey Formation along the Santa Barbara Channel. This configuration may have resulted from a series of fracturing events caused by an increase in remote tensile stress through time. The proposed model for cross joint development is based on stress perturbation in the vicinity of newly formed joints and assumptions on initial flaw size and distribution. A sequential infilling of joints occurs whereby cross joints propagate approximately at the midpoints between earlier generations of cross joints. Crack driving stress is reached first at midpoints since they experience the highest values of local tensile stress. The model proposes the first generation of cross joints initiating under remote tensile stress conditions ranging from approximately -13 to -16 MPa. The next set of cross joints propagates when the remote tensile stress reaches -27 MPa, followed by a third generation of cross joints at -57 MPa. While remote tensile stress increases with time, local stress within the mechanical layer follows a cyclical pattern, never exceeding the value for crack driving stress. The result of these three successive jointing events is the observed fracture spacing index of 1.30. Stress conditions for cross joint propagation may arise due to differential contraction of adjacent stratigraphic horizons during uplift and erosion of the Monterey Formation. Though non-systematic, cross joints are significant brittle features because they demonstrate that pre-existing joints can act as mechanical layer boundaries, indicate the role of layer-parallel stretching in the jointing process, may be used to calculate the magnitude of tensile stress near the earth's surface, and provide additional connectivity to fluid flow through a fractured rock mass.

Acknowledgements—I wish to thank T. Engelder, M. Fischer, P. Hancock and W. Narr for critically reviewing the manuscript, and R. Allmendinger for use of his stereonet program. Special thanks to W. Bartlett for field assistance and I. Aloni for statistical consulting. This work was supported by a research grant from Texaco Inc.

REFERENCES

Atkinson, B. K. 1987. Introduction to fracture mechanics and its geophysical applications. In: *Fracture Mechanics of Rock* (edited by Atkinson, B. K.). Academic Press, London, 1–26.

Atkinson, B. K. & Meredith, P. G. 1987. Experimental fracture mechanics data for rocks and minerals. In: *Fracture Mechanics of Rock* (edited by Atkinson, B. K.). Academic Press, London, 477–525.

Badgley, P. C. 1965. *Structural and Tectonic Principles*. Harper & Row, New York.

Burg, J. P. & Harris, L. B. 1982. Tension fractures and boudinage oblique to the maximum extension direction: an analogy with Lüders Bands. *Tectonophysics* **83**, 347–363.

Dibblee, T. W., Jr. 1950. Geology of southwestern Santa Barbara County, California. *Bull. Calif. Div. Mines & Geol.* **150**.

Dibblee, T. W., Jr. 1988a. Geologic map of the Solvang and Gaviota Quadrangles, Santa Barbara County, California. Dibblee Geological Foundation, map DF-16, scale 1:24,000.

Dibblee, T. W., Jr. 1988b. Geologic map of the Lompoc Hills and Point Conception Quadrangles, Santa Barbara, California. Dibblee Geological Foundation, map DF-18, scale 1:24,000.

Dyer, R. 1988. Using joint interactions to estimate paleostress ratios. *J. Struct. Geol* **10**, 685–699.

Engelder, T. & Lacazette, A. 1990. Natural hydraulic fracturing. In: *Rock Joints* (edited by Barton, N. & Stephansson, O.). *Proc. Int. Symp. Rock Joints*, 35–43.

Evans, K. F., Engelder, T. & Plumb, R. A. 1989. Appalachian stress study 1. A detailed description of in situ stress variations in Devonian shales of the Appalachian Plateau. *J. geophys. Res.* **94**, 129–7154.

Fleischmann, K. H. 1991. Interaction between jointing and topography: a case study at Mt Ascutney, Vermont, U.S.A. *J. Struct. Geol.* **13**, 357–361.

Garrett, K. W. & Bailey, J. E. 1977. Multiple transverse fracture in 90° cross-ply laminates of a glass fibre-reinforced polyester. *J. mater. Sci.* **12**, 157–168.

Gilbert, G. K. 1904. Domes and dome structure of the high Sierra. *Bull. geol. Soc. Am.* **15**, 29–36.

Ghosh, S. K. 1988. Theory of chocolate tablet boudinage. *J. Struct. Geol.* **10**, 541–553.

Gross, M. R. & Engelder, T. 1991. A case for neotectonic joints along the Niagara Escarpment. *Tectonics* **10**, 631–641.

Hancock, P. L. 1985. Brittle microtectonics: principles and practice. *J. Struct. Geol.* **7**, 437–457.

Hancock, P. L. & Engelder, T. 1989. Neotectonic joints. *Bull. geol. Soc. Am.* **101**, 1197–1208.

Helgeson, D. E. & Aydin, A. 1991. Characteristics of joint propagation across layer interfaces in sedimentary rocks. *J. Struct. Geol.* **13**, 897–911.

Hobbs, D. W. 1967. The formation of tension joints in sedimentary rocks: An explanation. *Geol. Mag.* **104**, 550–556.

Hodgson, R. A. 1961. Regional study of jointing in Comb Ridge–Navajo Mountain area, Arizona and Utah. *Bull. Am. Ass. Petrol. Geol.* **45**, 1–38.

Huang, Q. & Angelier, J. 1989. Fracture spacing and its relation to bed thickness. *Geol. Mag.* **126**, 355–362.

Isaacs, C. M., Pisciotto, K. A. & Garrison, R. E. 1983. Facies and diagenesis of the Miocene Monterey Formation, California. In: *Siliceous Deposits of the Pacific Region* (edited by Iijima, A., Hein, J. R. & Siever, R.). Elsevier, New York, 247–282.

Jahns, R. H. 1943. Sheet structures in granites: Its origin and use as a measure of glacial erosion in New England. *J. Geol.* **51**, 71–98.

Johnson, A. M. 1970. *Physical Processes in Geology*. Freeman, Cooper & Co., San Francisco.

Lachenbruch, A. H. 1961. Depth and spacing of tension cracks. *J. geophys. Res.* **66**, 4273–4292.

Ladeira, F. L. & Price, N. J. 1981. Relationships between fracture spacing and bed thickness. *J. Struct. Geol.* **3**, 179–183.

McQuillan, H. 1973. Small-scale fracture density in Asmari Formation of southwest Iran and its relation to bed thickness and structural setting. *Bull. Am. Ass. Petrol. Geol.* **57**, 2367–2385.

Narr, W. 1991. Fracture density in the deep subsurface: techniques with application to Point Arguello oil field. *Bull. Am. Ass. Petrol. Geol.* **66**, 1231–1247.

Narr, W. & Suppe, J. 1991. Joint spacing in sedimentary rocks. *J. Struct. Geol.* **13**, 1037–1048.

Pollard, D. D. & Segall, P. 1987. Theoretical displacements and stresses near fracture in rock: with applications to faults, joints, veins, dikes, and solution surfaces. In: *Fracture Mechanics of Rock* (edited by Atkinson, B. K.). Academic Press, London, 277–349.

Price, N. J. 1966. *Fault and Joint Development in Brittle and Semi-brittle Rocks*. Pergamon Press, Oxford.

Priest, S. D. & Hudson, J. A. 1976. Discontinuity spacings in rock. *Int. J. Rock. Mech. Min. Sci. & Geomech. Abs.* **13**, 135–148.

Segall, P. & Pollard, D. D. 1983. Joint formation in granitic rock of the Sierra Nevada. *Bull. geol. Soc. Am.* **94**, 563–575.

Senseny, P. E. & Pfeifle, T. W. 1984. Fracture toughness of sandstones and shales. *Proc. 25th U.S. Symp. Rock Mech.* Evanston, Illinois, 390–397.

Srivastava, D. C. & Engelder, T. 1990. Crack-propagation sequence and pore-fluid conditions during fault-bend folding in the Appalachian Valley and Ridge, central Pennsylvania. *Bull. geol. Soc. Am.* **102**, 116–128.

APPENDIX

Table A1. Cross joint spacing data from Alegria and Gaviota

Systematic joint pair (strike perpendicular joints) Locality,	Station,	Set	Mean MLT (spacing between systematic joints) (cm)	Mean spacing cross joints (cm)	Median spacing cross joints (cm)	Standard deviation	FSR MLT/Median	Number of joints
Gaviota	A	Set 1	42.60	30.92	31.50	7.63	1.35	8
Gaviota	A	Set 2	5.50	9.13	9.00	4.03	0.61	16
Gaviota	A	Set 3	30.70	26.54	24.80	9.31	1.24	11
Gaviota	A	Set 4	36.63	30.08	31.30	7.72	1.17	9
Gaviota	A	Set 5	42.87	30.94	26.60	8.68	1.61	11
Gaviota	A	Set 6	94.00	74.35	68.00	19.33	1.38	4
Gaviota	A	Set 7	1.50	2.74	2.50	0.95	0.60	22
Gaviota	B	Set 1	4.22	6.95	5.60	4.28	0.75	17
Gaviota	B	Set 2	33.40	33.54	34.00	6.21	0.98	11
Gaviota	B	Set 3	11.02	10.14	9.80	3.81	1.12	20
Gaviota	B	Set 4	7.06	5.81	6.10	1.64	1.16	20
Gaviota	B	Set 5	19.10	22.07	21.00	4.98	0.91	19
Gaviota	B	Set 6	12.00	10.88	10.15	3.31	1.18	34
Gaviota	B	Set 7	3.35	5.53	5.45	2.08	0.61	26
Gaviota	B	Set 8	7.23	9.38	9.80	3.23	0.74	26
Gaviota	B	Set 9	5.60	7.57	6.40	3.40	0.88	21
Gaviota	C	Set 1	21.50	25.15	24.60	7.41	0.87	26
Gaviota	C	Set 2	14.55	18.73	19.15	7.42	0.76	16
Gaviota	C	Set 3	34.00	31.95	31.00	8.34	1.10	29
Gaviota	C	Set 4	10.70	10.77	9.65	4.61	1.11	26
Alegria	A	Set 1	26.98	23.69	22.20	8.69	1.22	28
Alegria	A	Set 2	8.00	9.14	7.60	3.53	1.05	25
Alegria	A	Set 3	6.87	7.04	6.40	2.74	1.07	19
Alegria	A	Set 4	14.68	13.28	13.20	6.30	1.11	27
Alegria	A	Set 5	44.15	36.66	33.00	11.76	1.34	13
Alegria	A	Set 6	19.27	16.77	16.00	5.87	1.20	15
Alegria	A	Set 7	1.45	1.58	1.60	0.86	0.91	31
Alegria	B	Set 1	19.50	17.24	17.25	7.04	1.13	18
Alegria	B	Set 2	6.30	6.12	5.90	2.19	1.07	27
Alegria	B	Set 3	12.10	10.55	10.60	3.95	1.14	21
Alegria	B	Set 4	14.33	13.11	13.50	4.69	1.06	13
Alegria	B	Set 5	5.50	5.05	4.65	1.67	1.18	34
Alegria	B	Set 6	3.37	2.93	3.00	0.93	1.12	43
Alegria	B	Set 7	1.40	1.73	1.60	0.53	0.88	24

Note: FSR is the fracture spacing ratio, which corresponds to the mean mechanical layer thickness divided by the median joint spacing.